ADVANCED INTELLIGENT SYSTEMS
Open Access
www.advintellsyst.com

# A Soft Gripper with Granular Jamming and Electroadhesive Properties

*Yegor Piskarev,* Antoine Devincenti, Vivek Ramachandran, Pierre-Etienne Bourban, Michael D. Dickey, Jun Shintake, and Dario Floreano*

**In recent years, there has been a growing interest in the development of universal soft grippers that can handle objects of varying form factors (including flat objects), surface conditions (including moistened or oily objects), and mechanical properties (deformable and fragile). Yet, there is no single gripper that can gently grip objects with such a wide range of properties. Herein, a soft gripper that combines granular jamming (GJ) and electroadhesion (EA) to gently grasp and release a large set of diverse objects is presented. The gripper can operate in GJ mode only, in EA mode only, or in a combination mode that simultaneously activates GJ and EA. In GJ mode, the gripper can grasp objects with different surface properties, lift objects 38 times its own weight using negative pressure, and release objects by applying positive pressure, but has difficulty in handling flat and fragile objects. In EA mode, the gripper can manipulate flat and fragile objects but encounters difficulties with different surface properties such as oily or moisture. In the combination mode, the gripper can generate grasping forces up to 35% higher than in the GJ mode for all object sizes and certain shapes such as a cylinder. An interactive preprint version of the article can be found here: https://doi.org/10.22541/au.166937296.61200374/v1.**

## 1. Introduction

The softness of the human hand is a critical factor that allows us to hold, lift, and manipulate a variety of objects and has inspired roboticists to incorporate softness in gripper design and materials. The compliance of soft materials enables passive adaptation of the gripper during grasping operations, allowing manipulation of a wide range of objects without bringing additional control complexities.[1,2] In recent years, there has been growing interest in the development of universal soft grippers that can work with objects of different form factors, rigidity, surface properties, and level of fragility.[3–9] A possible approach to create such highly versatile grippers is to combine different gripping technologies that complement their individual limitations.[1,3,10–13] Yet, it is still challenging to develop a single gripper that can grasp and release objects of different form factors including flat objects, surface conditions (wet, porous, oily, and powdered), and mechanical properties (fragile and deformable).

In this article, we present a soft gripper capable of manipulating different objects with varying physical properties, such as shape, surface conditions, and rigidity. The proposed gripper combines two different technologies: granular jamming (GJ) to control stiffness and electroadhesion (EA) to control adhesion. Here we show that not only does this combination mutually compensate for the limitations of each individual technology, but it also makes the gripper capable of performing multistage grasping tasks that consist of diverse grasping and releasing operations on objects made of different materials, surfaces, and shapes. The manipulation of a book is an example of multistage operation that requires grasping and turning a rigid cover and flipping through single pages.

GJ enables reversible stiffness change between soft and rigid configurations by means of negative pressure.[5,14,15] High compliance in the soft state allows a GJ gripper to envelope the manipulated object by pressing on it. When negative pressure

Y. Piskarev, A. Devincenti, V. Ramachandran, D. Floreano
Laboratory of Intelligent Systems
Institute of Mechanical Engineering
School of Engineering
École Polytechnique Fédérale de Lausanne
1015 Lausanne, Switzerland
E-mail: yegor.piskarev@epfl.ch

The ORCID identification number(s) for the author(s) of this article can be found under https://doi.org/10.1002/aisy.202200409.



**DOI: 10.1002/aisy.202200409**

P.-E. Bourban
Laboratory for Processing of Advanced Composites
Institute of Materials
School of Engineering
École Polytechnique Fédérale de Lausanne
1015 Lausanne, Switzerland

M. D. Dickey
Department of Chemical and Biomolecular Engineering
North Carolina State University
911 Partners Way, Raleigh, NC 27695, USA

J. Shintake
Shintake Research Group
School of Informatics and Engineering
The University of Electro-Communications
1-5-1 Chofugaoka, Chofu, Tokyo 182-8585, Japan

is applied, the gripper becomes stiff and holds the encaged object.[2] GJ-based grippers are built as bistable systems: even small applied negative pressure has to trigger the stiffness change. Variable stiffness can also be achieved by integrating phase-change materials that have different mechanical properties at different temperatures.[10,16] However, GJ offers comparatively faster response time (≈100 ms), independence from environmental temperature, higher lifting force, easier fabrication, higher robustness, and lower cost.[2,5,17,18] The grasping force produced by GJ is sufficient to grasp objects of different morphologies, almost independently of the surface conditions of the object.[5,14,19] The grasping force of GJ grippers can vary from 0.09 to 1.2 kN.[15] GJ has been combined with soft pneumatic actuators to provide more dexterous grasp and lift heavier objects because of the enhanced holding forces.[13,20] However, GJ grippers cannot lift flat objects, such as a sheet of paper. Also, the grasping performance of delicate, fragile, and easily deformable objects such as a thin layer of cloth, an egg, or water balloons, as well as larger objects than the active area of the granular bag, can be challenging and has not been demonstrated so far.

EA instead is an adhesive technology that leverages the shear force generated by electrostatic forces.[21] Electroadhesive pads have been combined with different actuation technologies, such as dielectric elastomer actuation,[1] soft pneumatic actuation,[22] layer jamming,[23] and Fin-Ray-structured actuation.[24] The enhanced shear force makes EA-based grippers capable of delicately and rapidly (≈100 ms) grasping both flat and fragile objects without squeezing or breaking them.[1,2,25–29] While the adhesive force of EA pads can be tuned by regulating electrical input, EA effectiveness is highly dependent on the environmental and surface conditions of the object being grasped.[21] In particular EA is less effective for objects that are greasy, rough, or wet.[2] An additional challenge of soft grippers that rely on EA is the residual electrostatic charge that remains for a few seconds after removing the voltage and can result in difficult release of light objects.[30]

Here we present a new soft gripper that combines GJ and EA technologies to enhance and complement the grasping capabilities of each technology used in isolation. The soft gripper consists of an inflatable balloon filled with granules and an integrated electroadhesive pad with an interdigitated electrode structure (**Figure 1**a,b). This design enables activation of GJ and EA independently or in combination, thus offering three operation modes. In GJ mode, the gripper can hold and lift non-flat objects with negative air pressure (Figure 1d). Also, in GJ mode, the gripper can release objects by removing negative pressure or applying positive air pressure, which produces a convex curvature of the gripper's surface (Figure 1c). In EA mode, the gripper is capable of grasping flat and delicate objects by applying a voltage. In combined GJ and EA mode, the gripper can grasp and release a variety of objects with different geometries and surface conditions (moistened, oily, porous, and powdered). Moreover, the gripper is able to perform forced releasing of objects stuck on the device surface (e.g., sticky objects) by applying positive pressure that makes the gripper bulge outward.

We characterize the grasping performance of the gripper for different object sizes and analyze how grasping parameters such

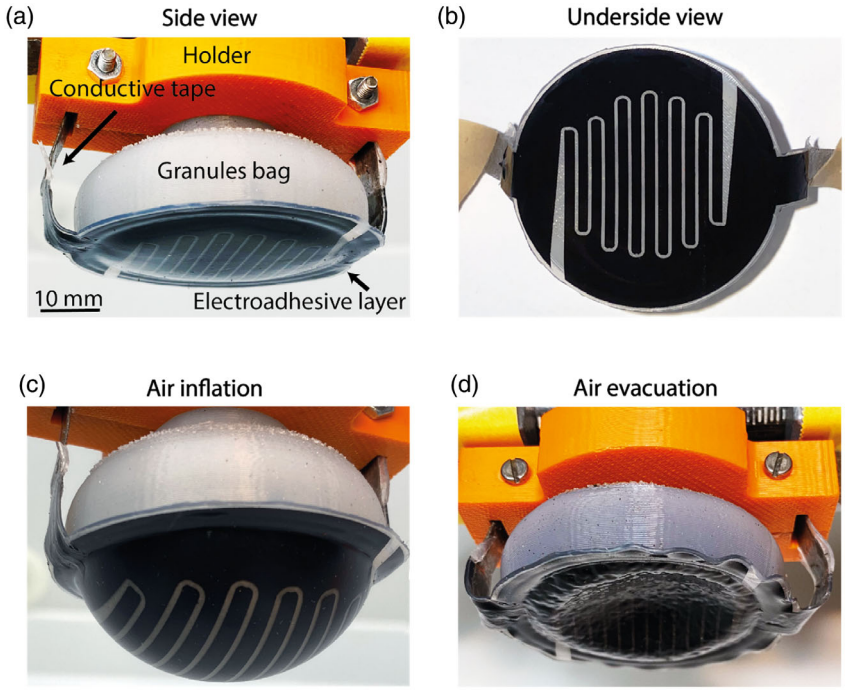


**Figure 1.** Structure of the gripper. a) The gripper consists of a silicone balloon with granules and a soft electrode layer at the bottom. The silicone bag is connected to an external vacuum pump and fixed by a holder. The electrode layer is plugged into an external power supply via conductive tape. b) The electrode layer consists of a circular interdigitated electrode structure made of conductive silicone. c) The gripper can change the geometry of the bottom layer from flat to hemisphere by applying a positive pressure via a vacuum pump. d) In the soft state, the gripper can take the shape of a grasped object (spherical object, as an example) and then maintain it after the air is evacuated.

as bending angle, applied force, and activation of GJ and EA influence the grasping force. We also assess the impact of the combined mode on the grasping of objects with different geometries and deformable objects, including flat objects of different sizes. We characterize the gripper's performance in picking up objects with different surface conditions determined by moisture, oiliness, porosity, and dust. Finally, we show the use of the gripper in multistage grasping tasks consisting of a sequence of different grasping and releasing operations. In one case, the gripper opens a rigid book cover in GJ mode and then gently flips pages in EA mode. In the other case, the gripper grasps a tea bag in EA mode, picks up a plastic cup in GJ mode, dips the tea bag into the plastic cup in EA mode, and finally releases the used tea bag by bulging out the gripper's surface in GJ mode.

## 2. Results and Discussion

### 2.1. Working Principle

The working principle of the dual gripper is illustrated in **Figure 2**. After reaching an object, one of the three different working modes can be activated (Figure 2a). Applying a high potential difference to the interdigitated electrode structure activates the EA gripper, causing fringing electric fields that extend from the surface of the gripper. These fields induce electric charges on the surface of the object (Figure 2b), resulting in the electrostatic adhesion force between the gripper and object.

The GJ mode relies on a bag filled with the granules, which is soft when the gripper approaches the target object (Figure 2c). As the gripper lowers against the object, the soft bag deforms and takes the shape of the object (Figure 2d); at this point, the bag is stiffened by evacuating the air and jamming the tightly packed granules (Figure 2e). This stiff state fixes the object against the bag such that it can be lifted. Pumping air back into the bag makes it soft by enabling movement of the granules, thereby causing the gripper to release the object (Figure 2f).

In the combined mode, the simultaneous activation of GJ and EA enhances the grasping force of the gripper. In the soft state, granules flow around the object increasing the contact surface between the object and the gripper. After activation GJ and EA, EA enhances the adhesive forces of the contact surface.[1,31]

### 2.2. Fabrication

The fabrication procedure consists of layer-by-layer and molding techniques, as illustrated in **Figure 3**. First, an EA pad was fabricated by encapsulating a conductive silicone layer with a laser-engraved interdigitated electrode in between two dielectric layers made of silicone (Figure 3a–i,ii,iii). All the layers were fabricated using a blade-casting technique and cured onto each other. Then, the fabricated EA pad was placed in an empty mold, which consists of an external, internal, and bottom part (Figure 3b–i). Liquid silicone was poured into the mold to form the silicone bag and connected the EA pad, resulting in a monolithic structure. After curing the silicone, the gripper was removed from the mold (Figure 3b–ii). Finally, the silicone bag was filled with coffee granules with diameters of 0.2 mm (Figure 3b–iii). A detailed explanation of the fabrication process is available in the Experimental Section. The resulting gripper had a weight of 13 g and the diameter of the grasping surface was 36 mm (the diameter of the interdigitated electrode structure was 30 mm).

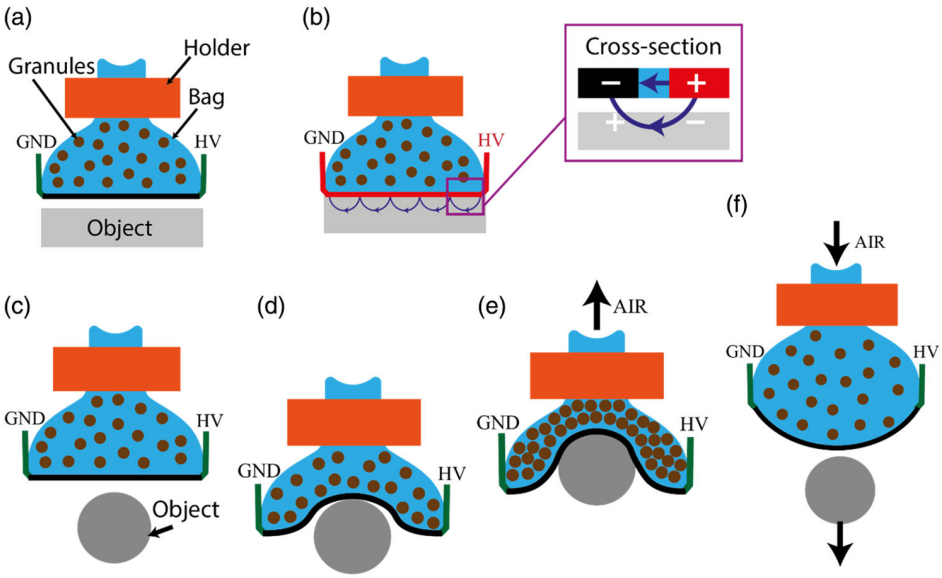


**Figure 2.** The gripper's schematic structure and operating principle of the gripper. a) The blue silicone balloon is held using an orange holder. Granules are kept inside the balloon. The electroadhesive pad is located on the bottom surface of the gripper and is connected to the ground and high-voltage electrodes. The gripper is lowered to the flat surface (in grey) of a grasping object. b) The applied potential difference causes the generation of electrostatic force attraction between the bottom surface of the gripper and the substrate surface of a grasping object. c–e) The working principle of a GJ mode. c) The gripper is lowered on an object. d) The gripper deforms and takes shape of the manipulated object. e) The air is evacuated by turning on the vacuum pump. f) The object can be released by applying positive pressure and changing the curvature of the bottom layer of the gripper.

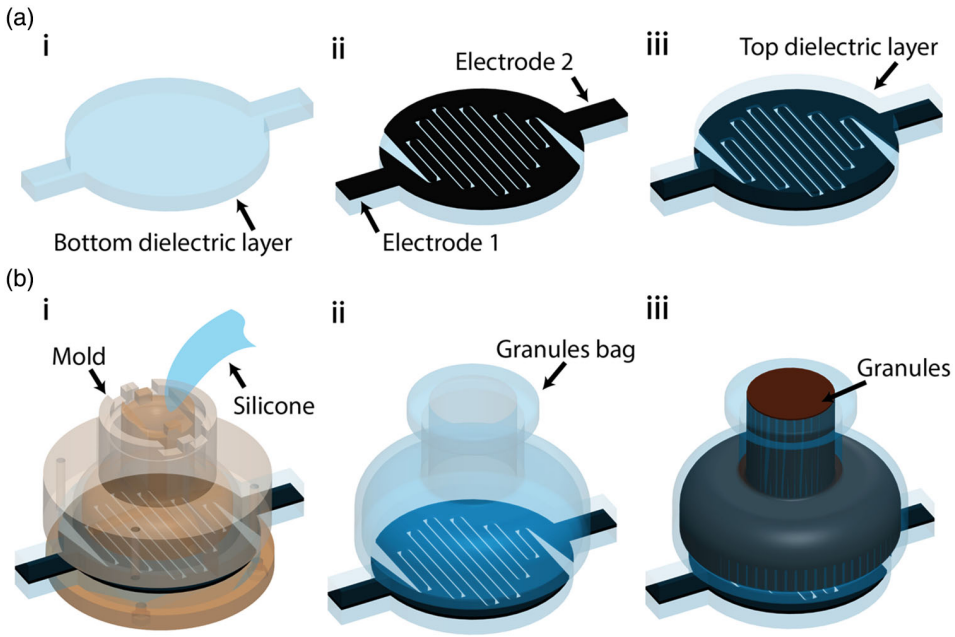


**Figure 3.** Fabrication process of the gripper. a) Electroadhesive pad fabrication. A three-layer structure, which consists of a bottom silicone layer i), a conductive silicone layer ii), and a top silicone layer iii), is blade cast and cured in an oven one on top of the other. The electrode pattern (ii) is engraved using $CO_2$ ablation before the top silicone layer (iii) is cast. b) i) The fabricated pad is placed in an empty mold. Then, liquid silicone is poured into the mold to form the silicone bag and simultaneously connect the bag and the pad in a monolithic structure. ii) The silicone is solidified by thermal curing and the gripper is removed from the mold. iii) The silicone bag is filled with coffee granules (in brown).

### 2.3. Grasping Force Characterization

The grasping performance of the gripper in GJ mode results from three different mechanisms: physical interlocking between the gripper and object, static friction caused by normal stresses in the contact regions, and suction effect due to a reduced air pressure over part of the contact surface (the latter can only occur when the gripper generates a vacuum seal against the object).[14] Static friction is the main factor because it contributes to both interlocking and suction modes.[5] Thus, the characterization of the grasping force of a GJ gripper is usually made for the static friction mechanism, which depends on the size and shape of the manipulated object, the contact angle, surface conditions, and applied force at the moment of grasp.[5,14]

In this study, the static friction mechanism in the combined mode is enhanced by EA, which increases the friction forces and normal forces of the gripper.[1,31] Thus, to quantify the grasping performance, we characterize the grasping force in GJ mode and in combined mode for different manipulated object sizes (**Figure 4**a). The gripper is connected to the tensile testing machine equipped with a load cell to perform vertical displacement and applied force measurements on the grasped object. The objects to be grasped are fixed on a plate beneath the gripper and in line with its central axis. The objects consist of a set of hemispheres printed in polylactic acid (PLA) with the diameters from 12 to 32 mm that correspond to 33–89% of the gripper diameter. The shape of the hemispheres does not allow interlocking grasp. The gripper is moved down to a preprogrammed height by the tensile machine and presses against the object (see Experimental Section). After that, the GJ or combined mode is activated, and the tensile machine lifts the gripper up until it releases the object. In the combined mode, the EA pad is activated by applying 2.5 kV and GJ is triggered by the air evacuation with a pressure drop of 84 kPa. Although the EA pad can operate up to 5 kV (Figure 4b), the applied voltage here is set to 2.5 kV to prevent possible breakdowns that may happen when squeezing the EA pad during the grasping operation. Based on the characteristics of shear forces at different voltages that were already studied for EA based,[22–24] we assume that the grasping force (i.e., the mass of object) of our gripper increases with increasing the applied voltage. The grasping force data for three experiments is collected using the load cell of the tensile machine.

In the GJ mode, the grasping force varies from 5.8 (standard deviation (SD) = 0.38 N) to 10.6 N (SD = 0.62 N) for object sizes from 33 to 89% of the gripper diameter. Interestingly, the maximum grasping force is achieved for the hemisphere with the size of 78% of the gripper diameter and then starts decreasing. In the case of combined mode, the grasping force varies from 6.1 (SD = 0.18 N) to 12.1 N (SD = 0.83 N) for object sizes from 33 to 89% of the gripper diameter. In this case, there is a continuous increase in grasping force with the size of the hemisphere. For the hemisphere size of 89% of the gripper diameter, the grasping force of the combined mode is 15.2% larger than the GJ mode's force.

In the GJ mode, the grasping force depends not only on the size of the object but also on the applied force with which a gripper touches the object. This applied force determines a contact angle between the gripper surface and the object. The contact angle and size of the object define the contact surface, that is., amount of granules in the contact zone between the gripper

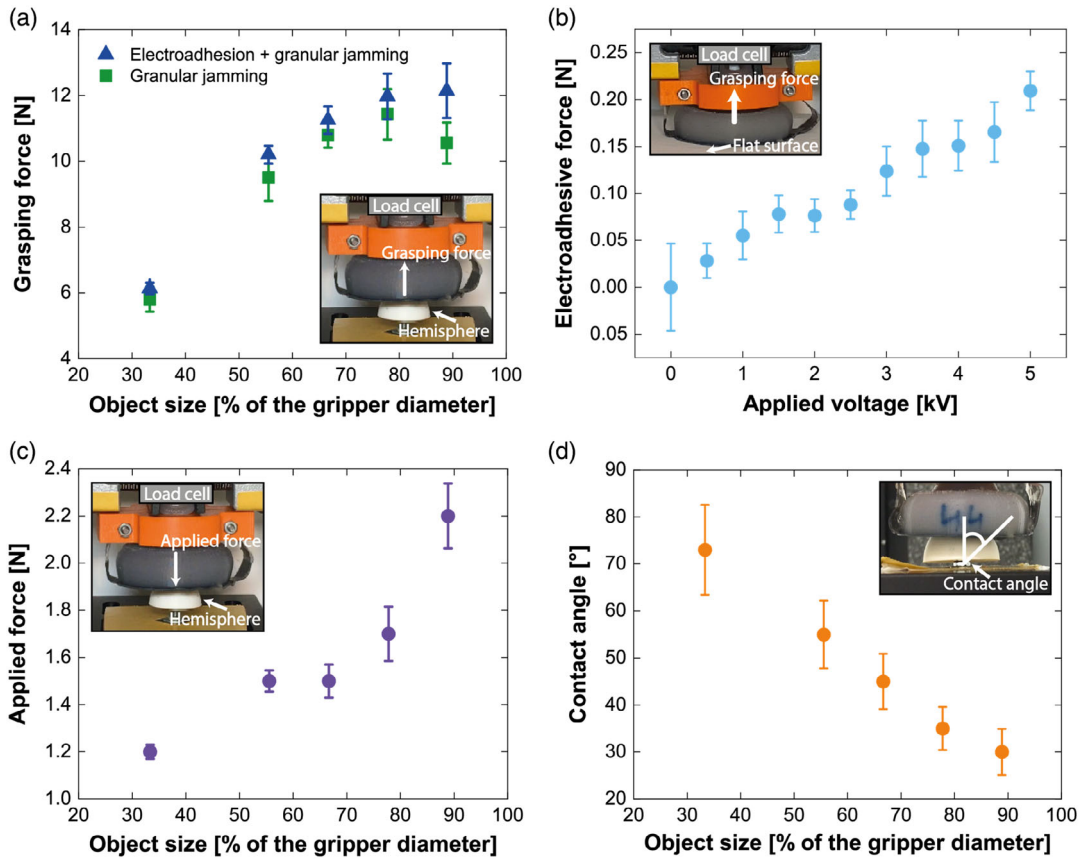


**Figure 4.** Characterization of grasping performance for an object with hemispheric shape. Each data point corresponds to the average measurement of three grippers tested five times each (15 measurements). a) Grasping force for GJ and combined (GJ with EA) modes as a function of object size. Diameters of hemispheres used in these tests range from 33% to 89% of the gripper's active area. The gripper was pushed down and contacted the hemisphere until it reached 5N of applied force in all experiments. In the combined mode, the EA pad was activated by applying 2.5 kV and GJ was triggered by the air evacuation with the pressure drop of 84 kPa. Grasping forces increase with increasing object diameter, but the combined mode displays 15.2% superiority for largest object diameter compared to GJ alone. b) The measured total EA force of the gripper as a function of applied voltages on a flat surface. The normal force scales from 0 to 0.2 N with the voltage applied from 0 to 5 kV with a step size of 500 V. c) The applied force as a function of a grasped object size. In experiments b and c, the gripper was pulled down to a certain absolute coordinate above all hemispheres. The applied force increases with the growth of the object size from 1.2 to 2.2 N. d) The contact angle as a function of a grasped object size. The contact angle changes from 73° to 30°.

and the object. To characterize the relationship between the applied force and the contact angle, we use the same setup with the tensile machine, hemispheres, and an additional camera placed in front of the gripper to capture the contact angle. The gripper is lowered to a preprogrammed height by the tensile machine. After reaching the hemisphere, the applied force data is collected from the load cell.

The applied force increases from 1.2 (SD = 0.03 N) to 2.2 (SD = 0.61 N) N for the object size from 33% to 89% of the gripper diameter (Figure 4c). The applied force grows with an increase of the object size because larger object size results in the larger contact surface area across which more granules can cover the target. We noticed that an increase in the applied force correlates with a decrease in the contact angle. We followed the commonly used way of representing contact angles for GJ-based grippers as an angle between the vertical line and the extreme contact point between a gripper and an object.[5,14] The lower contact angle shows that a larger area of the hemisphere is in the contact with the gripper causing more granules to flow toward the surface of the hemisphere, pressing onto it and resulting in a higher applied force. The contact angle decreases from 73° (SD = 9.6°) to 30° (SD = 4.9°) for the object size from 33% to 89% of the gripper diameter (Figure 4d).

The EA mode allows grasping of flat objects, which is not possible in GJ mode, by means of the normal force generated between the gripper and the object when voltage is applied. The amount of normal force generated by the interdigitated electrode structure depends on the design of electrodes, dielectric constants of contact materials, thickness of the dielectric layer, and effective area of contact. It also scales with the square of the applied voltage.[1,32] Other physical parameters, such as surface conditions and roughness, can also influence the normal force.[21] Thus, we performed experimental characterization of the EA-generated force (Figure 4b). The tensile machine lowers the gripper onto the flat surface and a voltage is applied from 0–5 kV with a step increment of 0.5 kV. The measured normal

force scales with the voltage as reported in the literature.[1,31,33] The inherent stiction between the outer dielectric layer and the flat surface causes high standard deviation of normal force measurements at zero voltage. Normal force reaches 0.2 N (SD = 0.02 N) at 5 kV. Normal force can also be enhanced either by decreasing the outer dielectric layer or increasing the density of generated fringe fields by decreasing the width of the electrodes and the gaps between electrodes.

The grasping force of conventional GJ grippers varies up to an order of magnitude depending on the shape of object.[5] Thus, we characterized the grasping force generated by the proposed gripper in GJ mode for different object geometries, including flat and deformable objects (**Figure 5**a). For these experiments, we used seven different 3D shapes with the cross-sectional diameter of 80–90% of the gripper's diameter, which corresponds to maximum grasping force (Figure 4a) consisting of a sphere, cube, pyramid, disks with 20 and 50 mm in a diameter, cylinder, and parallelepiped. All shapes were 3D printed with the highest layer thickness of 0.4 mm (instead of a usual 0.06 mm). The objects were fixed at the bottom of the tensile machine, while the gripper grasped and pulled the object up and measured the holding force. We tested three grippers three times for each shape. We observed the highest grasping forces of 6.1, 10.4, and 8.9 N in both modes for a sphere, cube, and disk of 20 mm. The combined mode increases the adhesion for these objects by 5.6%, 3.7%, and 0.5%. In comparison to spheres, these shapes

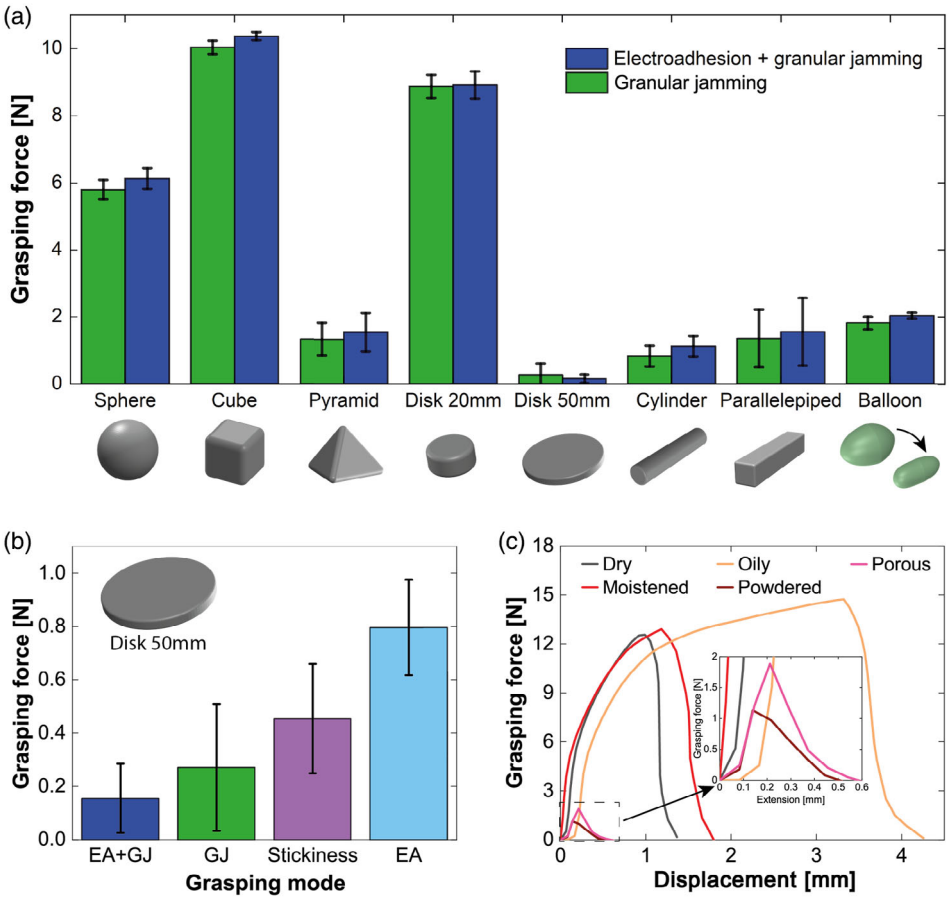


**Figure 5.** Characterization of grasping forces for different geometries and surface conditions. a) The grasping force for GJ and combined mode for different object geometries that have the same volume: sphere, cube, pyramid, disks with diameters of 20 and 50 mm, cylinder, parallelepiped, and deformable balloon with liquid. The flat disk with a diameter of 50 mm has a diameter larger than the diameter of a gripper and cannot be grasped using GJ mode. The highest grasping forces of 6.1, 10.4, and 8.9 N in both modes were observed for a sphere, cube, and disk of 20 mm. The combined mode increases the adhesion for these objects by 5.6%, 3.7%, and 0.5%. These shapes allow granules to flow more easily around the target object and grasp it from all sides. The highest differences of 35%, 16%, and 15% in grasping forces between GJ mode 0.83, 1.33, 1.35 N and combined mode 1.12, 1.54, 1.55 N are observed for a cylinder, pyramid, and parallelepiped, respectively. The combined mode shows worse performance only in the case of a disk of 50 mm (flat object). The activation of GJ in a combined mode makes the bottom surface involved in grasping rigid, thus, less compliant. b) Grasping forces of a flat object as a function of four grasping modes. EA mode (EA) shows the highest grasping force of 0.8 N compared to combined, GJ, and nature stickiness forces of 0.15, 0.27, and 0.45 N, resulting in the grasping enhancement of 430%, 194%, and 78%, respectively. c) The grasping force as a function of gripper's displacement for a combined mode for different surface conditions: dry (grey), oily (yellow), porous (pink), moistened (red), and powdered (brown). The hemisphere with the diameter of 28 mm, which corresponds to 78% of the gripper diameter, was used. The same setup and testing protocol as for Figure 4a was used. The grasping of objects with dry, moistened, and oily surfaces resulted in 4–5 times higher grasping force compared to porous and powdered surfaces due to suction effect formation.

allow granules to flow more easily around the target object and envelope it completely. Yet, when the manipulated object design is less suitable for GJ mode, the influence of EA on the resulted grasping force is higher. We observed the highest differences (35%, 16%, and 15%) in grasping forces between GJ mode (0.83, 1.33, 1.35 N) and combined mode (1.12, 1.54, 1.55 N) for a cylinder, pyramid, and parallelepiped respectively. In the case of deformable water balloon, we observed grasping forces of 1.8 and 2 N for the GJ and combined mode indicating the grasping enhancement of 11%. The illustration of the contact states between the gripper and the shapes during grasping can be found in Figure S2, Supporting Information.

We also characterized the grasping forces for each of the objects when GJ, EA, and the combined modes are turned off, and the object is lifted only due to the inherent stickiness of silicone (Figure S1, Supporting Information). Interestingly, for a flat object larger than the gripper size, we observed that two highest forces of 0.42 and 0.80 N are achieved in the soft state of the gripper using only the stickiness of silicone and EA mode, respectively (Figure 5b). In these modes, the gripper is in the soft state and is more compliant than GJ mode, resulting in a better contact between the gripper and the object that leads to higher grasping performance. The modes that include GJ, thus, stiff state of the gripper, result in the maximal grasping force of 0.27 N, which is three times lower than EA. The activation of GJ makes the gripper rigid and the external contact surface of the gripper becomes rough (Figure S3, Supporting Information). The higher surface roughness in a rigid state makes the contact area between the device and the manipulated object lower than in a soft state.[21]

Contrary to EA-based grippers, GJ-based grippers can grasp objects that are powdered, moistened, and porous.[14] In this study, we chose different gripper design and material composition from already existing devices.[34] Thus, we performed characterization of the grasping force at different surface conditions in the combined mode (Figure 5c) as this mode shows the highest grasping force among all modes (Figure 4a). We used the hemisphere with a diameter of 28 mm, which corresponds to 78% of the gripper diameter, following the same setup and testing protocol as for Figure 4a. We measure the grasping force for the gripper in combined mode under different surface conditions of the object: dry, oily, porous, moistened, and powdered. Porous and powdered surfaces result in the lowest grasping forces (1.1 and 1.9 N, respectively). Oily, moistened, and dry objects instead yielded substantially higher forces (14.8, 12.9, 12.6 N, respectively). The porous and powdered surfaces prevent the formation of the sealed interface between the gripper and object surfaces, eliminating the suction effect. In the case of oily, moistened, and dry objects, the silicone surface of the gripper fastens tightly around the object causing a suction effect, which magnifies the grasping force. These results are in line with the performance of a conventional GJ gripper measured with similar surface conditions.[14] These results indicate that the outer surface of the gripper, which is three times thicker than conventional GJ grippers due to the presence of the EA electrodes, does not limit grasping capabilities for different surface conditions.

### 2.4. Grasping and Manipulation of Fragile, Deformable, and Flat Objects

GJ is an effective method for grasping solid objects with different shapes.[5,14,15] However, the grasping of deformable and flat objects can be challenging and is never discussed in the literature for GJ-based grippers. Here we show that the combined use of GJ and EA enables successful pick and place of such objects (**Figure 6** and Video S1, Supporting Information). In a first example, we pick up two fragile quail eggs with diameters of 27 mm and a weight of 17 g each. The gripper in the soft state

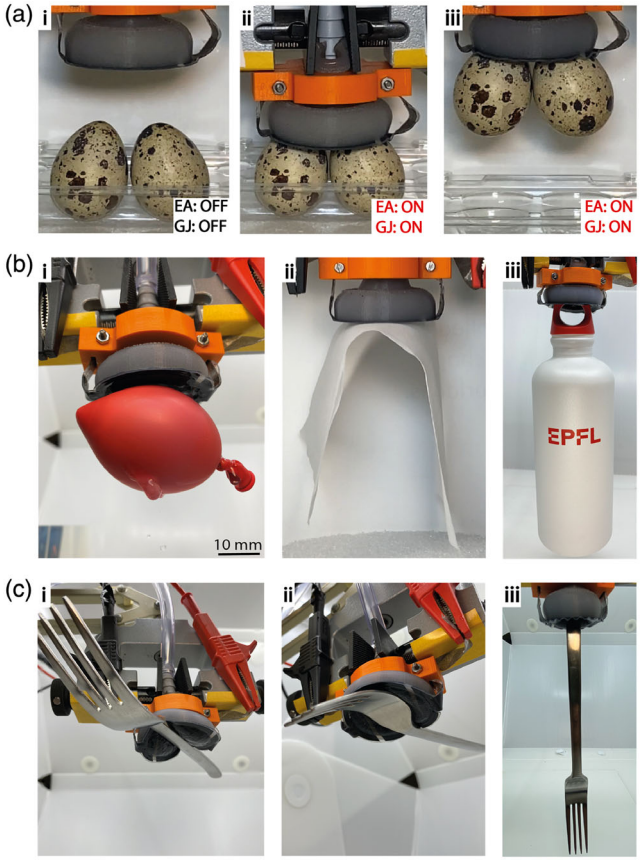


**Figure 6.** Working principle and grasping demonstration. a) Grasping is performed using a motorized linear stage, which raised and lowered the gripper. The gripper acts as an end effector (see Video S1, Supporting Information). i) In the initial state, a soft silicone bag with granules is soft. ii) When the gripper touches the object, the silicone bag deforms. After that, the pump and voltage are turned on. The pump evacuates the air out of the bag triggering the GJ and making it stiff to hold the object. The applied voltage (3 kV) triggers the generation of EA force on the bottom surface of the gripper. iii) The objects (two quail eggs with the weight of 34 grams) are then picked up due to the grasping force provided by the GJ and EA while the linear stage lifts up. Release of the objects is achieved by a reverse of the operating procedure explained above. b) With the same operating principle, a grasping demonstration is performed for i) a highly deformable water-filled balloon (31 g) ii) a flat and delicate fabric (0.5 g), and iii) a bottle with water (507 g). c) The high compliance of the gripper allows grasping objects from different sides broadening potential grasping scenarios. The fork (32 g) can be manipulated from three different sides (i–iii).

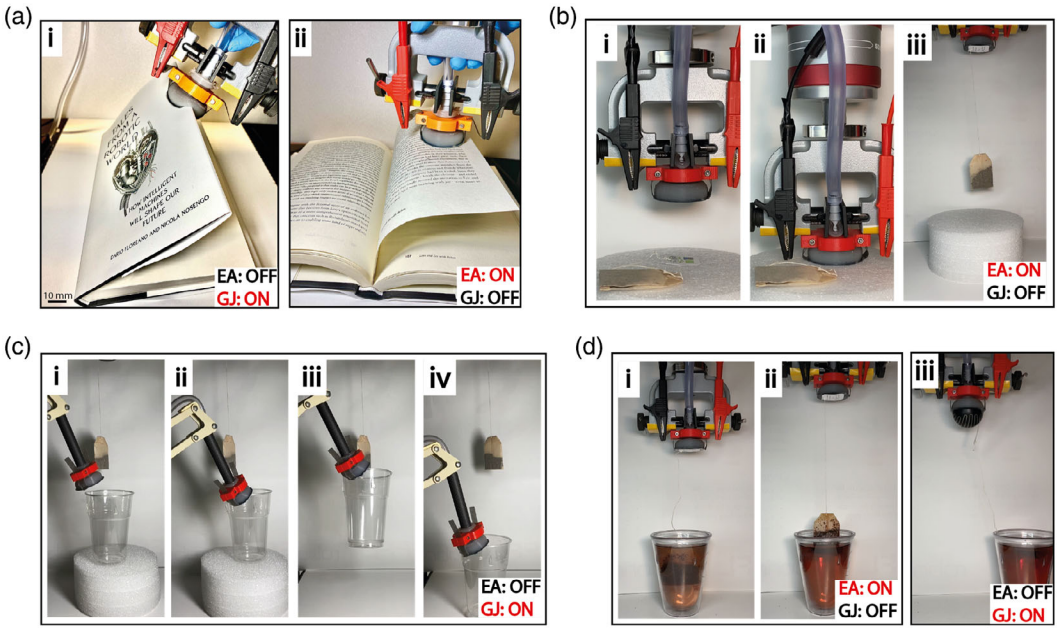


**Figure 7.** Demonstration of complex manipulation scenarios. Each black rectangular area corresponds to the use of a specific grasping mode: GJ or EA. a) The gripper can be used for complex manipulation such as an interaction with a book. i) The cover page can be opened by GJ mode. ii) Then, the pages can be gently turned over using EA mode. b) Another example of complex manipulation is tea making. i) The EA mode can be used to grasp i,ii) and lift iii) the teabag (1.8 g). c) The GJ mode of the second gripper is used to grasp i,ii), lift iii), and move iv) the plastic glass (8 g) for the tea. (d) i,ii) The teabag is moved up and down using linear stage. It changes the weight from 2 to 7.7 g when sopping. iii) The tea bag can be rapidly released by turning off EA and applying positive pressure to the gripper to change the curvature of the grasping surface and detach the object. The gripper can grasp objects with different surface conditions such as dry, oily porous, moistened, and powdered. The grasping force for dry, oily, and moistened objects are in 4–5 times higher compared to the objects with porous and powdered surfaces due to the formation of a tightly sealed interface between the gripper and the object surfaces, which leads to the suction effect.

approaches the eggs until the granules in the gripper flow around both eggs

(Figure 6a–i,ii); subsequently, the simultaneous activation of GJ and EA modes within 1 s allows the gripper to grasp the eggs (Figure 6a–ii) and lift them up (Figure 6a–iii). In a second example, we pick up a highly deformable water balloon with a size larger than the size of the gripper, a mass of 31 grams, and a membrane thickness less than 30 µm (Figure 6b–i). In a third example, we pick up a flat tissue with the weight of 0.5 g and thickness less than 60 µm, without deforming it (Figure 6b–ii). After lifting the tissue, the gripper can release it by applying positive pressure bulging out its surface (Video S1, Supporting Information). In a fourth example, we lift a bottle of water with a mass of 507 g, which is 38 times heavier than the gripper (Figure 6b–iii). In addition, the high deformability of the gripper allows it to grasp objects from different sides broadening potential grasping scenarios. In a fifth example, we pick up a fork of 32 g from three different sides (Figure 6c–i,ii,iii).

The ability to selectively operate in different modes allows the gripper to be used for multistage complex operations, such as opening and flipping through the pages of a book and making a cup of tea (**Figure 7** and Video S2 and S3, Supporting Information). In the first example, the book hardcover weighs ≈300 g (≈0.3 N) and requires GJ mode to open the book (Figure 7a–i); once the book is open, the pages can be gently flipped over in EA mode (Figure 7a–ii). In the second the EA mode can be used to grasp (Figure 7b–i,ii) and lift (Figure 7b–iii) a tea bag with a mass of 1.8 g. The GJ mode on the second gripper is used to grasp (Figure 7c–i,ii), lift (Figure 7c–iii), and move (Figure 7c–iv) the plastic glass with a mass of 8 g for the tea. Then, the tea bag is moved up and down (Figure 7d–i,ii) and changes the weight from 2 to 7.7 g as it absorbs water. The tea bag can be rapidly released by turning off EA and bulging out the gripper's surface by applying positive pressure (Figure 7d–iii).

## 3. Conclusion

We showed that the combination of controlled stiffness by GJ and controlled adhesion by EA can lead to versatile grippers capable of manipulating a broader range of objects than currently existing GJ-based, EA-based grippers, or their combination with other grasping technologies.[5,14,15,20,22–24] We combined GJ and EA together to exploit the grasping advantages of each technology. The fact that these technologies have the similar activation time range (0.1–1.1 s) and can be fabricated using the same soft materials in one monolithic structure also motivated us to combine them.[2] The gripper is fabricated out of commercially available and low-cost components such carbon black-filled elastomer composite and silicone elastomer using common fabrication techniques such as film casting, laser ablation, and molding.

The GJ mode allows lifting objects with a weight 38 times larger than the weight of the gripper. In addition, the application of positive pressure bulges out the gripper's surface to facilitate object release. The EA mode enables manipulation of flat and delicate objects, which would not be possible with GJ alone, with a weight of 20–80 g. On the other hand, GJ alone allows manipulation of objects with different surface conditions such as grease, oily, or moistened objects, which was not achieved by conventional EA grippers.[22–24] The grasping force in the combined mode, when GJ and EA are activated simultaneously, is higher for all the diameters of manipulated objects. The difference between combined mode of GJ & EA versus the pure GJ mode increases with the object sizes and achieves the maximum difference of 15.2% at the object size of 89% of the gripper's diameter. The generated grasping force correlates with the applied force before the gripper activation and inversely correlates with the grasping angle in the same manner shown in the literatures on conventional GJ grippers.[5,14] The gripper is capable of manipulating objects of various shapes. The combined mode shows the highest grasping force enhancement of 35%, 16%, and 15% compared to GJ for cylinder, pyramid, and parallelepiped shapes. The combined mode is especially beneficial with the shapes that do not allow granules to flow easily around the target object and grasp it from all sides.

The separate use of an EA, GJ, or combined modes makes the gripper suitable for complex manipulation scenarios that require manipulations of multiple objects with different sizes, shapes, softness, and surface conditions. In the future, the performance of EA pad can be improved by applying higher voltage and reducing the pressure applied onto the object while grasping. For industrial use, the gripper can be equipped with active cleaning elements to remove the dust from the EA pad, and the material of the gripper can be changed to industrial wear resistive to withstand high number of grasps. This gripper can be beneficial for agricultural applications where picking fresh vegetables and fruits without damaging them remains challenging.[35] Moreover, the gripper can be used to address current challenges in the industry such as the development of adaptive industrial assembly robots capable of manipulating objects in different ways such as twisting and regrasping with a large variety of different geometries.[36,37] The fabrication process of the gripper combines molding and layer-by-layer fabrication techniques that are both scalable. Thus, the proposed fabrication approach can easily be adapted to produce grippers with various dimensions suitable for the aforementioned applications.

## 4. Experimental Section

*Gripper Fabrication*: The silicone elastomer and carbon black-filled elastomer composite were fabricated out of conductive nanoparticles (AkzoNobel, Ketjenblack EC-300J) and a liquid silicone elastomer (Smooth-On, Ecoflex 00–30) in a planetary centrifugal mixer (Thinky, ARE-250) following the already existing manufacturing approach.[38] The fabrication of the gripper consisted of six steps. At the first step, the silicone layer for electroadhesive (EA) pad was prepared. The liquid silicone was poured onto a PET sheet and spread using an applicator coater (Zehntner, ZUA2000) and a variable-gap applicator (Zehntner, ZAA2300) with a gap of 100 μm and a drawing speed of 5 mm $s^{-1}$. The elastomer layer was then cured in an oven for 30 min at 80 °C. Then, in the second step, the conductive silicone layer was formed by pouring conductive silicone composite onto the silicon layer and blade casting it using a variable-gap applicator with the gap of 25 μm and a drawing speed of 15 mm $s^{-1}$. The multilayer sample was then placed in the oven for 60 min at 80 °C to form a thickness of conductive layer around 20 μm. In the third step, the electrode layer was ablated using a laser engraver (Trotec, Speedy 300) to obtain the interdigitated electrode structure (Figure 2a–ii), and then the sample surface was cleaned with a solvent (isopropyl alcohol) to remove etched conductive particles. Uncleaned regions with carbon particles will lead to a drastic decrease in the breakdown voltage of the pads. Conductive tape (3 M, 9713) was placed onto the electrodes from both sides to connect the device with the power supply after assembly. In the fourth step, the first step was repeated to encapsulate the interdigitated electrode structure. A variable-gap applicator with a gap of 1000 μm and a drawing speed of 5 mm $s^{-1}$ was used. In step five, liquid silicone was poured into the mold with the pad screwed to the bottom side of the mold. Then the silicone was left at least 2 h at room temperature to cure. Leaving it at room temperature also has the advantage to leave more time for the trapped air to emerge to the surface. In the sixth step, the coffee granules, which were already used in conventional GJ-based grippers,[5,14] with the diameter of 0.2 mm were poured into already fabricated silicone bag.

*Grasping Parameters and Grasping Force Characterization*: All the experiment the objects were 3D printed using a printer (Utimaker, S5) and polylactic acid (PLA) material (Ultimaker, Tough PLA) with the highest layer thickness of 0.4 mm (instead of a usual 0.06 mm). Porous hemisphere was made by drilling multiple through-holes to prevent airtight seal between the gripper and the manipulated object. All the objects had a screw hole on the bottom to ensure the connection between the object and the surface under the gripper in the linear stretcher (Instron, 5965). The gripper moved down with the speed of 1 mm $s^{-1}$ and stopped when the gripper's surface was 10 mm lower than the highest point of the manipulated object to ensure immersion of the object into granules from all the sides. After moving the gripper down, the force data form the load cell (Instron, EX2580-500N), which corresponds to applied force, was recorded. Then, the gripper was activated and moved up, while the force data was collected from the load cell of the linear stretcher. The GJ mode was activated using a vacuum pump (Thomas VTE 3), whose performance was measured using a manual pressure sensor. The pump was able to generate a pressure drop of 84 kPa, thus an absolute vacuum of 16 kPa considering the ambient pressure to be 100 kPa. This was close to the datasheet value of 15 kPa for absolute vacuum. The maximum generated force in each of the experiments was depicted and used to represent grasping force results. The grasping angle data was collected using a camcorder of the phone (IPhone, 6 s). Then, the data was manually processed. In the EA characterization, a flat sheet of paper was mounted on the bottom of the linear stretcher instead of the target object. The paper was chosen because it does not stick to the silicone bottom layer of the gripper.[1] A high-voltage supply (Stanford Research Systems, PS350/5000 V–25 W) was used to activate the devices. The power applied to the EA pad was 0.25 W (2500 V, 0.1 mA). A low-capacity load cell (Instron, EX2580-10N) was used to measure the grasping forces.

## Supporting Information

Supporting Information is available from the Wiley Online Library or from the author.

## Acknowledgements

The authors thank Euan John Kenneth Judd for helpful comments and discussions. This work was supported by the SNSF Bridge project 20B2-1 180861 and JSPS KAKENHI Grant-in-Aid for Scientific Research on Innovative Areas "Science of Soft Robot" project (grant number 21H00324).

 

## Conflict of Interest

The authors declare no conflict of interest.

## Data Availability Statement

The data that support the findings of this study are available from the corresponding author upon reasonable request.

## Keywords

electroadhesion, granular jamming, soft grippers, soft robotics universal grippers

Received: November 23, 2022
Revised: February 7, 2023
Published online:

[1] J. Shintake, S. Rosset, B. Schubert, D. Floreano, H. Shea, *Adv. Mater.* **2016**, *28*, 231.
[2] J. Shintake, V. Cacucciolo, D. Floreano, H. Shea, *Adv. Mater.* **2018**, *30*, 1707035.
[3] Y.-F. Zhang, N. Zhang, H. Hingorani, N. Ding, D. Wang, C. Yuan, B. Zhang, G. Gu, Q. Ge, *Adv. Funct. Mater.* **2019**, *29*, 1806698.
[4] T. T. Hoang, P. T. Phan, M. T. Thai, N. H. Lovell, T. N. Do, *Adv. Mater. Technol.* **2020**, *5*, 2000724.
[5] J. R. Amend, E. Brown, N. Rodenberg, H. M. Jaeger, H. Lipson, *IEEE Trans. Rob.* **2012**, *28*, 341.
[6] V. Subramaniam, S. Jain, J. Agarwal, P. Valdivia y Alvarado, *Int. J. Rob. Res.* **2020**, *39*, 1668.
[7] C. Tawk, A. Gillett, M. In het Panhuis, G. M. Spinks, G. Alici, *IEEE Trans. Rob.* **2019**, *35*, 1268.
[8] C. Tawk, E. Sariyildiz, G. Alici, *Soft Rob.* **2022**, *9*, 970.
[9] G. Alici, N. N. Huynh, *IEEE/ASME Trans. Mechatron.* **2007**, *12*, 73.
[10] D. McCoul, S. Rosset, N. Besse, H. Shea, *Smart Mater. Struct.* **2016**, *26*, 025015.
[11] J. Shintake, B. Schubert, S. Rosset, H. Shea, D. Floreano, in *2015 IEEE/RSJ Int. Conf. on Intelligent Robots and Systems*, IEEE, New York, **2015**, pp. 1097–1102.
[12] N. G. Cheng, M. B. Lobovsky, S. J. Keating, A. M. Setapen, K. I. Gero, A. E. Hosoi, K. D. Iagnemma, in *IEEE Inte. Conf. on Robotics and Automation* **2012**, pp. 4328–4333.
[13] Y. Wei, Y. H. Chen, T. Ren, Q. Chen, C. X. Yan, Y. Yang, Y. T. Li, *Soft Rob.* **2016**, *3*, 134.
[14] E. Brown, N. Rodenberg, J. Amend, A. Mozeika, E. Steltz, M. R. Zakin, H. Lipson, H. M. Jaeger, *Proc. Natl. Acad. Sci.* **2010**, *107*, 18809.
[15] J. Miettinen, P. Frilund, I. Vuorinen, P. Kuosmanen, P. Kiviluoma, *Proc. Est. Acad. Sci.* **2019**, *68*, 421.
[16] E. Piskarev, J. Shintake, V. Ramachandran, N. Baugh, M. D. Dickey, D. Floreano, *Adv. Intell. Syst.* **2020**, *2*, 2000069.
[17] G. D. Howard, J. Brett, J. O'Connor, J. Letchford, G. W. Delaney, *Soft Rob.* **2021**, *9*, 497.
[18] S. Eristoff, S. Y. Kim, L. Sanchez-Botero, T. Buckner, O. D. Yirmibeşoğlu, R. Kramer-Bottiglio, *Adv. Mater.* **2022**, *34*, 2109617.
[19] C. E. Capalbo, D. Tomaino, F. Bruno, D. Rizzo, B. Phillips, S. Licht, *IEEE J. Oceanic Eng.* **2022**, *47*, 975.
[20] L. Al Abeach, S. Nefti-Meziani, T. Theodoridis, S. Davis, *J. Bionic Eng.* **2018**, *15*, 236.
[21] P. Rajagopalan, M. Muthu, Y. Liu, J. Luo, X. Wang, C. Wan, *Adv. Intell. Syst.* **2022**, *4*, 2200064.
[22] J. Guo, K. Elgeneidy, C. Xiang, N. Lohse, L. Justham, J. Rossiter, *Smart Mater. Struct.* **2018**, *27*, 055006.
[23] R. Chen, Z. Zhang, J. Guo, F. Liu, J. Leng, J. Rossiter, *Soft Rob.* **2021**, *9*, 1074.
[24] R. Chen, R. Song, Z. Zhang, L. Bai, F. Liu, P. Jiang, D. Sindersberger, G. J. Monkman, J. Guo, *Soft Rob.* **2019**, *6*, 701.
[25] H. Jiang, E. W. Hawkes, C. Fuller, M. A. Estrada, S. A. Suresh, N. Abcouwer, A. K. Han, S. Wang, C. J. Ploch, A. Parness, M. R. Cutkosky, *Science Rob.* **2017**, *2*, eaan4545.
[26] S. Song, D.-M. Drotlef, C. Majidi, M. Sitti, *Proc. Natl. Acad. Sci.* **2017**, *114*, E4344.
[27] V. Cacucciolo, J. Shintake, H. Shea, in *2019 2nd IEEE Int. Conf. on Soft Robotics (RoboSoft)*, IEEE, Piscataway NJ **2019**, pp. 108–113.
[28] V. Cacucciolo, H. Shea, G. Carbone, *Extreme Mech. Lett.* **2022**, *50*, 101529.
[29] K. M. Digumarti, V. Cacucciolo, H. Shea, in *2021 IEEE/RSJ Int. Conf. on Intelligent Robots and Systems (IROS)*, IEEE, Piscataway NJ **2021**, pp. 6104–6109.
[30] G. J. Monkman, P. M. Taylor, G. J. Farnworth, *Int. J. Cloth. Sci. Technol.* **1989**, *1*, 14.
[31] S. Park, J. Shintake, Y. Piskarev, Y. Wei, I. Joshipura, E. Frey, T. Neumann, D. Floreano, M. D. Dickey, *Adv. Mater. Technol.* **2021**, *6*, 2100263.
[32] H. A. Pohl, *J. Appl. Phys.* **1958**, *29*, 1182.
[33] R. Liu, R. Chen, H. Shen, R. Zhang, *Int. J. Adv. Rob. Syst.* **2013**, *10*, 36.
[34] J. M. Gómez–Paccapelo, A. A. Santarossa, H. D. Bustos, L. A. Pugnaloni, *Granular Matter* **2020**, *23*, 4.
[35] B. Zhang, Y. Xie, J. Zhou, K. Wang, Z. Zhang, *Comput. Electron. Agric.* **2020**, *177*, 105694.
[36] N. Rahman, L. Carbonari, M. D'Imperio, C. Canali, D. G. Caldwell, F. Cannella, American Society of Mechanical Engineers Digital Collection, **2016**.
[37] J. Hughes, K. Gilday, L. Scimeca, S. Garg, F. Iida, *Intell. Serv. Rob.* **2020**, *13*, 169.
[38] J. Shintake, E. Piskarev, S. H. Jeong, D. Floreano, *Adv. Mater. Technol.* **2018**, *3*, 1700284.